

The electric field induced ferroelectric phase transition of AgNbO₃

Hiroki Moriwake, Ayako Konishi, Takafumi Ogawa, Craig A. J. Fisher, Akihide Kuwabara, and Desheng Fu

Citation: *Journal of Applied Physics* **119**, 064102 (2016); doi: 10.1063/1.4941319

View online: <http://dx.doi.org/10.1063/1.4941319>

View Table of Contents: <http://scitation.aip.org/content/aip/journal/jap/119/6?ver=pdfcov>

Published by the [AIP Publishing](#)

Articles you may be interested in

Domain configuration changes under electric field-induced antiferroelectric-ferroelectric phase transitions in NaNbO₃-based ceramics

J. Appl. Phys. **118**, 054102 (2015); 10.1063/1.4928153

Unique dielectric tunability of Ag(Nb_{1-x}Tax)O₃ (x=0–0.5) ceramics with ferroelectric polar order

Appl. Phys. Lett. **104**, 182902 (2014); 10.1063/1.4875581

Electric field induced metastable ferroelectric phase and its behavior in (Pb, La)(Zr, Sn, Ti)O₃ antiferroelectric single crystal near morphotropic phase boundary

Appl. Phys. Lett. **104**, 052912 (2014); 10.1063/1.4864317

Phenomenological theory of electric-field-induced phase transition behavior of antiferroelectric ceramic (Pb,Ba,La)(Zr,Sn,Ti)O₃ under uniaxial compressive pre-stress

J. Appl. Phys. **112**, 034112 (2012); 10.1063/1.4744010

Phase diagram of pseudobinary Pb (Yb 1/2 Nb 1/2) O 3 – Pb (Sc 1/2 Nb 1/2) O 3 ceramic solid solution

J. Appl. Phys. **97**, 013527 (2005); 10.1063/1.1819977

The new SR865 2 MHz Lock-In Amplifier ... \$7950



Chart recording



FFT displays



Trend analysis

Features

- Intuitive front-panel operation
- Touchscreen data display
- Save data & screen shots to USB flash drive
- Embedded web server and iOS app
- Synch multiple SR865s via 10 MHz timebase I/O
- View results on a TV or monitor (HDMI output)

Specs

- 1 mHz to 2 MHz
- 2.5 nV/√Hz input noise
- 1 μs to 30 ks time constants
- 1.25 MHz data streaming rate
- Sine out with DC offset
- GPIB, RS-232, Ethernet & USB

SRS Stanford Research Systems
www.thinkSRS.com · Tel: (408)744-9040

The electric field induced ferroelectric phase transition of AgNbO₃

Hiroki Moriwake,^{1,a)} Ayako Konishi,¹ Takafumi Ogawa,¹ Craig A. J. Fisher,¹ Akihide Kuwabara,¹ and Desheng Fu²

¹Nanostructures Research Laboratory, Japan Fine Ceramics Center, Nagoya 456-8587, Japan

²Department of Electronics and Materials Sciences, Shizuoka University, Hamamatsu 432-8561, Japan

(Received 12 November 2015; accepted 21 January 2016; published online 10 February 2016)

Coexistence of two phases of AgNbO₃ is shown to explain the experimentally observed polarization–electric field hysteresis loop better than either phase in isolation, based on detailed first-principles calculations of the structural changes and stabilities of different phases of this compound. Calculations confirm a ferroelectric phase transition, whereby the symmetry of the AgNbO₃ crystal switches from antiferroelectric *Pbcm* to ferroelectric *Pmc2₁*, under an electric field of 9 MV/cm. The calculated spontaneous polarization (0.61 C/m²) under this field compares well with the experimental value of 0.52 C/m². After transforming, the structure remains in the ferroelectric state even after the electric field is removed, despite the structure being energetically metastable. As the energy difference between the antiferroelectric and ferroelectric phases is only +0.5 meV/f.u. and the potential energy barrier between them (~40 meV/f.u.) is comparable to thermal fluctuation energies, it is possible for these two phases to coexist at temperatures well below the paraelectric–antiferroelectric transition temperature (~626 K). The exploitation of this phenomenon in AgNbO₃ and related materials may provide a useful strategy for developing high-performance piezoelectric materials. © 2016 AIP Publishing LLC. [<http://dx.doi.org/10.1063/1.4941319>]

I. INTRODUCTION

Perovskite-structured silver niobate is an attractive candidate for developing lead-free piezoelectric materials to replace widely used lead zirconate titanate. The pure phase, AgNbO₃, exhibits ferroelectric behavior at room temperature, with a large polarization of 52 μC/cm² and a large electric field-induced strain under a high electric field of 220 kV/cm.¹ The subtle modifications in atom positions and crystal symmetry associated with this ferroelectric behavior mean, however, that the precise structural mechanisms responsible for its ferroelectricity are still not fully understood.

As with many perovskite-type oxides, AgNbO₃ undergoes a complex series of phase changes as a function of temperature and pressure. Above 852 K, AgNbO₃ is paraelectric, with a cubic (*Pm* $\bar{3}$ *m*) symmetry; as temperature is lowered, it transforms sequentially to paraelectric tetragonal (*P4/mbm*) and orthorhombic (*Cmcm*) phases, followed by two antiferroelectric phases and one ferroelectric orthorhombic phase below 626 K.^{2,3} For the high-temperature phases (above 626 K), the crystal structures are well characterized, but in the low temperature region, the precise structures of antiferroelectric and ferroelectric phases are less clear, with different space groups proposed by different research groups. These so-called M₁, M₂, and M₃ phases were investigated by Sciau *et al.*² using neutron powder diffraction and single-crystal X-ray diffraction; they assigned the centrosymmetric *Pbcm* space group to the average of the M₁, M₂, and M₃ structures, since they could not identify any significant structural differences between them. The weak room temperature ferroelectric behavior was attributed to local defects such as

Ag vacancy clustering. Levin *et al.*³ also reported that the ferroelectric phase has a *Pbcm* symmetry and attributed its ferroelectricity to local cation displacement disorder. Recently, Yashima *et al.*,^{4,5} as well as Chang *et al.*,⁶ proposed space group *Pmc2₁* for the ferroelectric phase based on the results of electron diffraction, neutron, and synchrotron powder diffraction experiments. Clarification of the different symmetries of the ferroelectric and antiferroelectric phases and their relative stabilities is an essential step in understanding the phase transition mechanisms in this system and should help hasten the development of new and improved ferroelectric materials.

First-principles calculations within the framework of density functional theory (DFT)^{7,8} represent an alternative and complementary means of probing ferroelectric phase transitions in materials at the atomic level. As well as allowing detailed comparison of crystal and electronic structures of the ferroelectric and antiferroelectric phases, first-principles methods can be used to identify the soft-mode phonon associated with a given phase transition.^{9–11} First-principles calculations of AgNbO₃ have been used by Grinberg and Rappe,¹² Shigemi and Wada,¹³ Yashima *et al.*,^{4,5} and Niranjana and Asthana¹⁴ to compare the relative energetics and polarizations of antiferroelectric and ferroelectric candidate structures. As with the above mentioned works, Niranjana and Asthana found a very small energy difference between the *Pbcm* and *Pmc2₁* phases (only 0.1 meV/f.u.). To explain the experimental hysteresis loop, which exhibits antiferroelectric-like behavior with a small remnant polarization at zero field, they concluded by suggesting that the ferroelectric phase coexists within the parent antiferroelectric *Pbcm* phase. More recently, we reported first-principles phonon calculations of the ferroelectric and antiferroelectric

^{a)}Author to whom correspondence should be addressed. Electronic mail: moriwake@jfcc.or.jp

structures of AgNbO_3 , showing that a soft-mode is absent over all wave vectors for both, indicating that the antiferroelectric $Pbcm$ phase has a dynamically stable structure.¹⁵ The ferroelectric behavior of AgNbO_3 thus cannot be explained simply as a spontaneous structural transition from the $Pbcm$ phase. Although lattice expansion is known to often stabilize otherwise energetically unfavorable ferroelectric phases, even under a static tensile pressure up to -6 GPa, the $Pbcm$ phase was calculated to remain dynamically stable, further confirming that the ferroelectric phase transition is not soft mode-related.¹⁵ Following the suggestion of Sciau *et al.*² that defects may be responsible for the ferroelectricity, we also examined point defect formation in this compound as a possible origin of its ferroelectric behavior and found that there should be an abundance of Ag vacancies and O vacancies in AgNbO_3 crystals.¹⁶ However, these and all previous calculations were performed with the crystal under zero electric field, and the possibility that the ferroelectric phase transition of AgNbO_3 is electrically induced was not considered. In this study, we examine the structural changes that take place under an electric field using DFT methods to see how this affects the ferroelectric behavior.

II. METHODOLOGY

All DFT calculations were performed within the revised Perdew–Burke–Ernzerhof exchange model of the generalized gradient approximation (GGA-PBE),¹⁷ using the plane-wave basis pseudopotential method. The polarization–electric field (P - E) diagram was constructed by optimizing structures under various constant electric fields using the ABINIT code.^{18,19} For the norm-conserving pseudopotentials,²⁰ 2s and 2p electrons for O, 4s, 4p, 4d, and 5s electrons for Nb, 4d, and 5s electrons for Ag were explicitly treated as valence electrons. A plane-wave cutoff energy of 544 eV was used. Numerical integration was carried out using $3 \times 3 \times 2$ k -point mesh for 40-atom unit cells within Brillouin zones generated by the Monkhorst–Pack scheme.²¹ The convergence with respect to the number of k points was better than that of the cutoff energy. The relaxation procedure was terminated when all the residual forces on the atoms were smaller than 0.05 eV/Å. The potential energy surface between the antiferroelectric and ferroelectric structures was calculated using the nudged elastic band (NEB) method as implemented in VASP.^{22,23} The conditions used in NEB calculations were set similar to those used for structure optimization.

III. RESULTS AND DISCUSSION

Figure 1(a) shows the optimized structure of the antiferroelectric $Pbcm$ phase in the absence of an electric field. This structure is in good agreement with the room temperature structure determined experimentally (within the usual DFT error). Previous high-precision phonon calculations confirmed that this structure has no soft vibrational modes.¹⁵ The ferroelectric $Pmc2_1$ structure determined from experiment^{4,5} corresponds to atomic displacements parallel to the b axis of the $Pbcm$ phase. We thus applied an electric field, E , along this direction; the resulting ferroelectric structure is shown in Figure 1(b). Under a sufficiently large electric field,

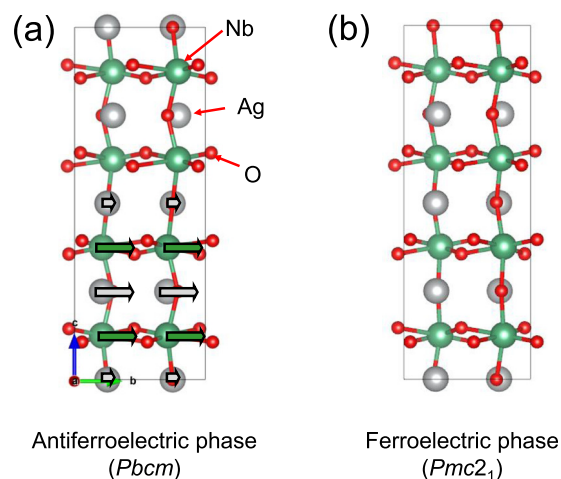


FIG. 1. Crystal structures of AgNbO_3 : (a) antiferroelectric $Pbcm$ phase and (b) ferroelectric $Pmc2_1$ phase. The atomic displacements under an electric field are shown in panel (a). Displacement of the ions under a finite electric field reduces the symmetry from $Pbcm$ to $Pmc2_1$. Loss of centrosymmetry in the $Pmc2_1$ phase causes AgNbO_3 to become ferroelectric.

cations are displaced in the positive (+) direction, while oxygen atoms are displaced in the negative (–) direction, resulting in a decrease in symmetry from space group $Pbcm$ to $Pmc2_1$. The loss of centrosymmetry gives the $Pmc2_1$ structure its ferroelectric characteristics.

The calculated P - E hysteresis loop is shown in Fig. 2. In the lower electric field region, linear polarization (structure) changes occurred. However, at around 9 MV/cm, a discontinuous change was observed. Most importantly, after the electric field was removed, the ions in the crystal did not return to their original (antiferroelectric) $Pbcm$ positions. Even under zero electric field, the crystal remained ferroelectric with $Pmc2_1$ symmetry and a relatively large spontaneous polarization of 0.49 C/m^2 , in excellent agreement with the experimental value of 0.52 C/m^2 .¹ The calculated structural parameters listed in Table I are also in good agreement with the experimental values of Yashima *et al.*⁴ Comparison of the total energy of the antiferroelectric phase with that of the ferroelectric $Pmc2_1$ phase shows that the latter is slightly less stable ($+0.5 \text{ meV/f.u.}$), consistent with Niranjana and Asthana's report.¹⁴

Figure 2 shows that the polarization becomes saturated at around 0.61 C/m^2 , close to the measured value of 0.52 C/m^2 .¹ However, at other points, the theoretical and experimental hysteresis loops are not in such good agreement. Experimentally,

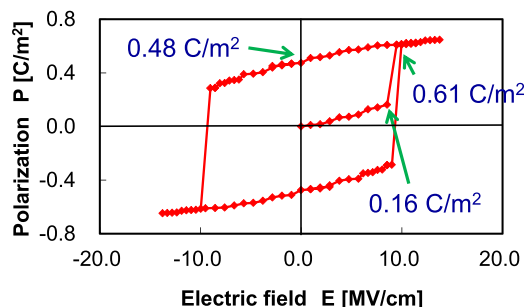


FIG. 2. Calculated P - E hysteresis loop for AgNbO_3 .

TABLE I. Crystal structure of the ferroelectric ($Pmc2_1$) phase of $AgNbO_3$.

Parameter	Theoretical			Experimental (Ref. 4)		
a	15.649 Å			15.648 Å		
b	5.644 Å			5.552 Å		
c	5.709 Å			5.609 Å		
Site	x	y	z	x	y	z
Nb1	0.875	0.256	0.286	0.875	0.242	0.236
Nb2	0.625	0.756	0.769	0.625	0.753	0.782
Ag1	0.751	0.746	0.259	0.750	0.747	0.255
Ag2	0.000	0.765	0.268	0.000	0.742	0.240
Ag3	0.500	0.264	0.766	0.500	0.253	0.778
O1	0.750	0.306	0.229	0.752	0.297	0.232
O2	0.860	0.960	0.033	0.866	0.959	0.035
O3	0.638	0.035	0.944	0.642	0.016	0.976
O4	0.890	0.533	0.463	0.885	0.543	0.464
O5	0.611	0.456	0.519	0.606	0.481	0.521
O6	0.000	0.192	0.249	0.000	0.191	0.259
O7	0.500	0.799	0.712	0.500	0.804	0.719

an antiferroelectric-like P - E hysteresis loop with a very small remnant polarization of 0.05 C/m^2 is observed;¹ in other words, the samples exhibit both ferroelectric and antiferroelectric behavior. This complexity can be rationalized by considering the energetics of the transition between the two low-temperature ($Pbcm$ and $Pmc2_1$) structures obtained from NEB calculations.

The calculated potential energy surface traced by $AgNbO_3$ in transforming from $Pbcm$ to $Pmc2_1$ symmetry is shown in Fig. 3. This potential surface features a double-well, one side corresponding to the $Pbcm$ phase and the other to the $Pmc2_1$ phase, with a potential barrier height of 40 meV/f.u. In other words, under zero electric field, the antiferroelectric $Pbcm$ phase is the ground-state structure of this compound, but the ferroelectric $Pmc2_1$ phase, while corresponding to a metastable structure, is only slightly less energetically stable. Because this energy difference is the same order of magnitude as thermal vibration energies at normal temperatures ($\sim kT$), it is possible for the ferroelectric phase to coexist with the ground state antiferroelectric phase, as first suggested by Niranjana and Asthana.¹⁴ Such a mixed system can explain the smaller remnant polarization and overall shape of the experimental P - E hysteresis loop observed by experiment.

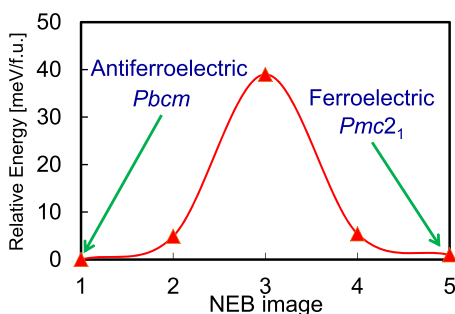


FIG. 3. Potential surface within $AgNbO_3$ during the ferroelectric phase transition from $Pbcm$ to $Pmc2_1$ under a finite electric field.

It is worth pointing out that coexistence of ferroelectric and antiferroelectric phases in single domains has also recently been reported by Shimizu *et al.* for the perovskite-type solid solution $x\text{CaZrO}_3-(1-x)\text{NaNbO}_3$ ($0 \leq x \leq 0.1$), which exhibits a similar double hysteresis loop to $AgNbO_3$, based on combined results from experiment and first-principles calculations.²⁴ Mixed antiferroelectric-ferroelectric domains at room temperature may thus be a feature of other perovskite niobate-related systems, pointing the way to the design of new lead-free ferroelectric materials.

IV. CONCLUSIONS

A systematic and quantitative analysis of the structures and energetics of the ferroelectric phase transition of $AgNbO_3$ under a finite electric field was carried out using first-principles calculations, and the results are compared with recent experimental findings.¹ The main results can be summarized as follows:

- (1) Under a high electric field, the room-temperature antiferroelectric $AgNbO_3$ $Pbcm$ crystal undergoes a phase transformation to the ferroelectric $Pmc2_1$ structure. The transition voltage is estimated to be 9 MV/cm .
- (2) The ferroelectric $Pmc2_1$ phase is slightly higher in energy ($+0.5 \text{ meV/f.u.}$) than the antiferroelectric phase. The potential surface between the two structures has a double-well feature with a potential barrier height of 40 meV/f.u. , so that under zero electric field the antiferroelectric $Pbcm$ phase is the ground-state structure and the ferroelectric $Pmc2_1$ structure is metastable. However, at finite temperatures (e.g., room temperature) below the antiferroelectric-paraelectric phase transition, the ferroelectric phase is expected to coexist with the ground-state antiferroelectric phase as thermal fluctuations are sufficient to overcome the small energy barrier. A mixture of $Pmc2_1$ and $Pbcm$ phases can explain the observed double hysteresis loop at room temperature.

ACKNOWLEDGMENTS

This work was supported by the Ministry of Education, Culture, Sports, Science and Technology of Japan through the Grants-in-Aid for Scientific Research (C) 24560833 and a Grant-in-Aid for Scientific Research on Innovative Areas “Nano Informatics” (Grant No. 25106008) from the Japan Society for the Promotion of Science (JSPS) and the Green Network of Excellence (GRENE).

¹D. Fu, M. Endo, H. Taniguchi, T. Taniyama, and M. Itoh, *Appl. Phys. Lett.* **90**, 252907 (2007).

²Ph. Sciau, A. Kania, B. Dkhil, E. Suard, and A. Ratuszna, *J. Phys.: Condens. Matter* **16**, 2795 (2004).

³I. Levin, V. Krayzman, J. C. Woicik, J. Karapetrova, T. Proffen, M. G. Tucker, and I. M. Reaney, *Phys. Rev. B* **79**, 104113 (2009).

⁴M. Yashima, S. Matsuyama, R. Sano, M. Itoh, K. Tsuda, and D. Fu, *Chem. Mater.* **23**, 1643 (2011).

⁵M. Yashima and S. Matsuyama, *J. Phys. Chem. C* **116**, 24902 (2012).

⁶H. Chang, M. Shang, C. Zhang, H. Yuan, and S. Feng, *J. Am. Ceram. Soc.* **95**, 3673 (2012).

⁷P. Hohenberg and W. Kohn, *Phys. Rev.* **136**, B864 (1964).

⁸W. Kohn and L. J. Sham, *Phys. Rev.* **140**, A1133 (1965).

- ⁹H. Moriwake, C. A. J. Fisher, A. Kuwabara, H. Taniguchi, M. Itoh, and I. Tanaka, *Phys. Rev. B* **84**, 104114 (2011).
- ¹⁰H. Taniguchi, H. P. Soon, T. Shimizu, H. Moriwake, Y. J. Shan, and M. Itoh, *Phys. Rev. B* **84**, 174106 (2011).
- ¹¹H. Moriwake, C. A. J. Fisher, A. Kuwabara, and T. Hashimoto, *Jpn. J. Appl. Phys., Part 1* **50**, 09NE02 (2011).
- ¹²I. Grinberg and M. Rappe, in *Fundamental Physics in Ferroelectrics*, edited by P. K. Davis and D. J. Singh (American Institute of Physics, 2003), p. 130.
- ¹³A. Shigemi and T. Wada, *Mol. Simulat.* **34**, 1105 (2008).
- ¹⁴M. K. Niranjan and S. Asthana, *Solid State Commun.* **152**, 1707 (2012).
- ¹⁵H. Moriwake, C. A. J. Fisher, A. Kuwabara, and D. Fu, *Jpn. J. Appl. Phys., Part 1* **51**, 09LE02 (2012).
- ¹⁶H. Moriwake, C. A. J. Fisher, A. Kuwabara, and D. Fu, *Jpn. J. Appl. Phys., Part 1* **52**, 09KF08 (2013).
- ¹⁷J. P. Perdew, K. Burke, and M. Ernzerhof, *Phys. Rev. Lett.* **77**, 3865 (1996); **78**, 1396 (1997).
- ¹⁸X. Gonze, J.-M. Beuken, R. Caracas, F. Detraux, M. Fuchs, G.-M. Rignanese, L. Sindic, M. Verstraete, G. Zerah, F. Jollet, M. Torrent, A. Roy, M. Mikami, Ph. Ghosez, J.-Y. Raty, and D. C. Allan, *Comput. Mater. Sci.* **25**, 478 (2002).
- ¹⁹I. Souza, J. Iniguez, and D. Vanderbilt, *Phys. Rev. Lett.* **89**, 117602 (2002).
- ²⁰A. M. Rappe, K. M. Rabe, E. Kaxiras, and J. D. Joannopoulos, *Phys. Rev. B* **41**, 1227 (1990).
- ²¹H. J. Monkhorst and J. D. Pack, *Phys. Rev. B* **13**, 5188 (1976).
- ²²G. Mills, H. Jonsson, and G. K. Schenter, *Surf. Sci.* **324**, 305 (1995).
- ²³G. Kresse and J. Furthmüller, *Phys. Rev. B* **54**, 11169 (1996).
- ²⁴H. Shimizu, H. Guo, S. E. Reyes-Lillo, Y. Mizuno, K. M. Rabe, and C. A. Randall, *Dalton Trans.* **44**, 10763 (2015).